AD-A173 631 IONIC MECHANISMS OF SOOT FORMATION IN FLAMES(U) 1/1
AEROCHEM RESEARCH LABS INC PRINCETON NJ
H F CALCOTE ET AL APR 86 AEROCHEM-TP-456
UNCLASSIFIED AFOSR-TR-86-1062 F49620-83-C-0150 F/G 21/2 NL

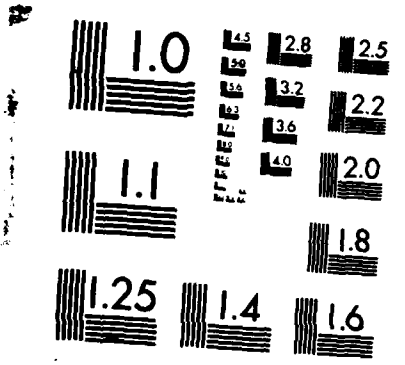

AFOSR-TR- 86-1062

(2)

AeroChem TP-456

IONIC MECHANISMS OF SOOT FORMATION IN FLAMES

H.F. Calcote and D.G. Keil
AeroChem Research Laboratories, Inc.
P.O. Box 12
Princeton, New Jersey 08542

April 1986

Annual Report for Period 15 September 1984 to 30 June 1985

Prepared for:
Air Force Office of Scientific Research
Bolling Air Force Base
Washington, DC 20332

UNCLASSIFIED
SECURITY CLASSIFICATION OF THIS PAGE

AD-A173 631

REPORT DOCUMENTATION PAGE

1a. REPORT SECURITY CLASSIFICATION: Unclassified	1b. RESTRICTIVE MARKINGS: None
2a. SECURITY CLASSIFICATION AUTHORITY	3. DISTRIBUTION/AVAILABILITY OF REPORT: Approved for public release, distribution unlimited
2b. DECLASSIFICATION/DOWNGRADING SCHEDULE	
4. PERFORMING ORGANIZATION REPORT NUMBER(S): TP-456	5. MONITORING ORGANIZATION REPORT NUMBER(S): AFOSR-TR- 86-1062
6a. NAME OF PERFORMING ORGANIZATION: AeroChem Research Laboratories, Inc. / 6b. OFFICE SYMBOL (If applicable)	7a. NAME OF MONITORING ORGANIZATION: Air Force Office of Scientific Research
6c. ADDRESS (City, State and ZIP Code): P.O. Box 12, Princeton, New Jersey 08542	7b. ADDRESS (City, State and ZIP Code): Bolling Air Force Base, DC 20332-6448
8a. NAME OF FUNDING/SPONSORING ORGANIZATION: Air Force Office of Scientific Research / 8b. OFFICE SYMBOL (If applicable): AFOSR/NA	9. PROCUREMENT INSTRUMENT IDENTIFICATION NUMBER: F49620-83-C-0150
8c. ADDRESS (City, State and ZIP Code): Bolling Air Force Base, DC 20332-6448	10. SOURCE OF FUNDING NOS.

PROGRAM ELEMENT NO.	PROJECT NO.	TASK NO.	WORK UNIT NO.
61102F	2308	A2	

11. TITLE (Include Security Classification): Ionic Mechanisms of Soot Formation in Flames

12. PERSONAL AUTHOR(S): H.F. Calcote and D.G. Keil

13a. TYPE OF REPORT	13b. TIME COVERED	14. DATE OF REPORT (Yr., Mo., Day)	15. PAGE COUNT
Annual	FROM 9/15/84 TO 6/30/85	1986 April	

16. SUPPLEMENTARY NOTATION

17. COSATI CODES			18. SUBJECT TERMS (Continue on reverse if necessary and identify by block number)
FIELD	GROUP	SUB. GR.	
21	01		Soot Formation; Ionic Mechanism; Flame Measurements
21	02		

19. ABSTRACT (Continue on reverse if necessary and identify by block number)

The mass range of ions sampled from low pressure (2.7 kPa) acetylene-oxygen flames was extended to approximately 600 amu which made it necessary to calibrate the mass spectrometer mass scale. This was done by adding salts to the feed gases and by using deuterated acetylene as fuel. These experiments also allowed determination of the number of hydrogen atoms in a given ion, from which the structures of the flame ions up to mass 559 were deduced. Mass spectra were obtained for ten acetylene-oxygen flames with equivalence ratios of 1.0 to 3.0. The possibility that the large ions observed in sooting flames are derived from heating of small growing soot particles by exothermic surface reactions was examined theoretically. Although the necessary data for such a calculation are not accurately known, a temperature of soot particles about 100 K above the gas temperature was calculated. Equilibrium ionization of soot particles with this temperature enhancement could not account for the observed degree of ionization.

20. DISTRIBUTION/AVAILABILITY OF ABSTRACT	21. ABSTRACT SECURITY CLASSIFICATION
UNCLASSIFIED/UNLIMITED ☒ SAME AS RPT. ☐ DTIC USERS ☐	Unclassified

22a. NAME OF RESPONSIBLE INDIVIDUAL	22b. TELEPHONE NUMBER (Include Area Code)	22c. OFFICE SYMBOL
Julian M. Tishkoff	(202) 767-4935	AFOSR/NA

DD FORM 1473, 83 APR — EDITION OF 1 JAN 73 IS OBSOLETE.

UNCLASSIFIED
SECURITY CLASSIFICATION OF THIS PAGE

TABLE OF CONTENTS

LIST OF TABLES

LIST OF FIGURES

I INTRODUCTION

For a number of years the personnel at AeroChem have been protagonists of the ionic mechanism of soot formation in flames. In this theory, it is assumed that chemi-ions grow very rapidly through a series of ion-molecule reactions to produce large ions which are neutralized to produce either very small incipient soot particles, or very large neutral molecules which rapidly grow to form the incipient soot particles. We have, in fact, previously demonstrated that there is no sharp demarcation between large molecules and small soot particles.[1,2] After much study by many people, an understanding of the soot nucleation process still represents one of the more significant problems challenging the combustion community. A large part of the reason for this is that the necessary data required to resolve the many questions about the initial stages of soot formation--where the major questions apply--are very difficult to obtain experimentally; global measurements of soot particles do not give the necessary information. The objective of our program has been to make the necessary detailed ion (both total and individual) concentration profile measurements in the same flames in which Howard and associates at MIT[3-6] and others, e.g., Delfau and associates[7-9] in France and Homann and associates in Germany[10-13] are making complementary measurements. Our measurements include: mass spectrometer measurements for individual ion concentrations; Langmuir probe measurements for total ion concentrations; and temperature compensated thermocouple measurements for temperature profiles. To assure that the flames we study are exactly comparable to those used by Howard and associates at MIT, we have duplicated their burner.

During this reporting period we were honored by an invitation to present our work on the ionic mechanism of soot formation at the Gordon Conference on Fuels. As a theme we used: "Why I Believe In The Ionic Mechanism Of Soot Formation In Flames". The evidence was reviewed there in detail; for the record it is summarized in Table I.

The work statement for this program contained two phases. Phase I experiments are to be done in well studied flames of benzene-oxygen and acetylene-oxygen and they include generation of temperature profiles, Langmuir probe curves of total ion concentration, and mass spectrometer profiles of individual ions. Phase II involves model development of the individual processes involved in incipient soot formation, e.g., rates of ion and particle formation, rates of production of large molecular ions, the temperature of the growing particle and its effect on thermal ionization, thermal ionization of large molecules, and ion molecule rate coefficients. The quantitative models developed in this program for each of the steps will form the basis for a detailed overall quantitative model of the total process of soot formation. Considerably more time was consumed in the calibration of the mass scale than anticipated but this was necessary in order to treat the problem quantitatively. This was done at the expense of other experimental tasks.

In this report we summarize the results on this program during this report period. Result which have been published will be only briefly summarized; other results will be covered in more detail.

II. RESEARCH STATUS

A. APPARATUS

The apparatus used in the mass spectrometric studies reported here consists of a multitubular burner supported on a vertical translation stage which feeds through a vacuum seal into a cylindrical flame chamber pumped by a large (140 $L \cdot s^{-1}$) mechanical pump. The top of the chamber is fitted with a water-cooled plate supporting a metal sampling cone which permits the sampling of flame gases through an (0.013-0.025 cm) orifice into the first of two differentially pumped vacuum chambers. This chamber, maintained at less than 0.01 Pa pressure, contains a series of electrostatic lenses which focus and direct the flame ion beam into the second vacuum chamber containing a quadrupole mass filter, maintained at pressures below 0.001 Pa by a 15 cm (6 in.) diffusion pump. The quadrupole used in this work was constructed at AeroChem about 20 years ago. In this study it was powered by a 350 kHz rf supply providing a useful mass range up to nearly 600 amu. Ions which pass through the mass filter strike the cathode of an electron multiplier and the amplified current is recorded on an XY recorder as a function of mass (fixed burner position) or as a function of burner position (fixed ion mass).

The copper burner used by Bittner and Howard[5] at MIT was duplicated[14] so we could compare our ion profiles with their profiles of neutral species in the same flames.

During this report period we acquired a digitizer pad so that we could transfer mass spectrometer data from recorder charts to a computer for processing.

B. MASS SPECTROMETER MASS CALIBRATION

Because we extended the mass spectrometer range to fairly high mass ranges, approaching 600 amu, it was necessary to calibrate the mass range. This calibration was, in fact, complicated by the high range because no good standard ions are available in this range. Normally, the introduction into the flame of easily ionized alkali metal salts provides unambiguous mass markers in the hot flame gases. In this case, the salts of potassium (39 and 41 amu), rubidium (85 and 87 amu), cesium (133 amu), and lead (206 and 208 amu) were useful only in the low mass region. Due to strong nonlinearity of the mass scale below 50 amu and more subtle nonlinearity in other ranges, reliable extrapolations to 600 amu were not feasible even with the use of the above salts and the many known hydrocarbon masses below about 250 amu previously observed in rich acetylene-oxygen flames with greater mass resolution.[7,15] In order to identify the masses of the many heavy ions observed beyond 200 amu,

we recorded and compared the spectra from fuel rich deuterated acetylene flames. In order to conserve the isotopic fuel, a smaller burner was selected for the calibration experiments. This burner was similar to the stainless steel burner used in previous studies[15-17] except that the central tubes were fed gases separately from the outer tubes which gave a 2.64 cm central burner surrounded by a 4.70 cm o.d. annular burner. The annular flame (C_2H_2/O_2) provided a simple and rapid way to switch gases in the central burner and quickly reignite the test flames (C_2H_2/O_2 or C_2D_2/O_2). Once the central flame became stable, the annular flame was extinquished to avoid diffusional mixing of protonated and deuterated species. Attempts to stabilize 50 cm/s (unburned gas velocity) flames at 2.67 kPa were fruitless on this small diameter burner, so a velocity of about 80 cm/s was selected which provided stable flames at an equivalence ratio of 2.5 to 2.6. These flames are rich in ions throughout the mass range of the spectrometer.

The C_2D_2, was produced from the reaction of D_2O (99.8% D, Stohler Isotope Chemicals) with calcium carbide. The C_2D_2 passed through a drying tube into a 5 L storage vessel. After this vessel was filled to 1 atm, the generation was terminated and the vessel connected to a calibrated sonic orifice flowmeter. The C_2D_2 was fed to the burner at a constant rate by metering nitrogen into a balloon in the storage vessel to maintain a constant pressure (about 90 kPa absolute) upstream of the 0.025 cm orifice. The downstream pressure was always small enough to ensure sonic flow. The orifice calibration with C_2H_2 was used for the C_2D_2 by making a small correction for the mass difference. Comparison of mass spectra from C_2H_2 and C_2D_2 flames showed a general one-to-one correspondence for the peaks in the same general pattern of relative intensities; the deuterated ion peaks were shifted to higher mass by a difference that generally increased for larger ions.

The initial mass assignments were based on the distance in the recorded spectra between the well-characterized $C_3H_3^+$ (and K^+: 39 amu) and $C_{13}H_9^+$ (165 amu) ion peaks. Although this did not give the correct masses elsewhere, it provided a common mass scale for which a mass correction function could be developed. It also provided an approximation to the true mass scale for comparing the isotopic peaks. For example, any peaks that coincide on this scale must be identical in mass. The strategy was to correct the mass scale for known masses, e.g., alkali metals, apply the correcting equation to the "raw" spectra, and then compare the protonated and deuterated flame spectra. The hydrogen content of an ion is given by the shift upon deuteration, while the remaining mass indicates the number of carbon atoms and the possible presence of oxygen, the only other element in the flame.

Mass assignments were made to be consistent with: low mass hydrocarbon ions identified in previous work,[7,15] alkali metal and lead ions; and several integer mass relationships, ΔM, between the ions observed in the two isotopic flames. For adjacent species, $C_xO_yH_z^+$ and $C_x'O_y'H_z'^+$ (and the deuterated analogs):

$$\Delta M_H = 12(X'-X) + 16(Y'-Y) + (Z'-Z) \qquad \text{protonated}$$

$$\Delta M_D = 12(X'-X) + 16(Y'-Y) + 2(Z'-Z) \qquad \text{deuterated}$$

$$\Delta M_{N\,D} = Z \qquad \text{inter-isotope}$$

$$\Delta M_{N}{}'_{D}{}' = Z' \qquad \text{inter-isotope}$$

The analysis was complicated by the low mass spectrometer resolution used for high throughput: single ion peaks had widths on the order of 2 amu, increasing to 4 amu at higher masses. Mass peaks observed at every carbon number from 3 to 45 (the high mass limit of the instrument), appeared as single peaks in the protonated spectra, but many became multiple peaks upon deuteration.

A change in the number of hydrogen atoms in adjacent peaks is indicated by a consistent set of mass changes. For example, if adjacent peaks differed by CH_2 then $\Delta M_N = 14$, $\Delta M_D = 16$, and $\Delta M_{N\,D}' - \Delta M_{N\,D} = 2$. The restrictions on the values of these separations provide a method to monitor the changing hydrogen content of the ions throughout the mass spectrum, one carbon number at a time. Ambiguities were resolved through consideration of the effect of multiple, overlapping mass peaks. An example is provided by the peaks corresponding to C_{35} and C_{36} which were simulated as sums of simple Gaussians in Fig. 1. Each of the ion species will exhibit a significant ^{13}C ion peak with intensity, relative to the pure ^{12}C ion, proportional to the number of carbon atoms, e.g., 1.1% per carbon atom. Each observed peak was then treated as the sum of contributions from ion species differing in the number of hydrogen (deuterium) atoms and their respective ^{13}C isotope peaks. The symbols represent the experimental profiles of the adjacent C_{35} and C_{36} peaks from the C_2H_2 flame (Fig. 1a) and the C_2D_2 flame (Fig. 1b). The apparent single peaks in Fig. 1a are compared with the obviously multiple peaks in the C_2D_2 flame (Fig. 1b). The sparse lines represent calculated profiles for individual ions which sum up to yield the heavy line matching the experimental data. The following constraints were observed: (1) Individual ion peaks (e.g., $C_{35}H_y$) were approximated as Gaussians with widths (FWHM) of 4 amu and adjustable amplitudes, I_0. As drawn in the figure, each peak also includes the contribution from the ^{13}C isotopic ions at 1 amu higher mass and (from the number of carbon atoms) a statistically calculated intensity of 0.4 I_0. (2) The mass scale (amu/chart distance) had the same value for both Fig. 1a and 1b. (3) The chemical formulas of all the individual ions were identical for the two flames. In this case, the formulas in Fig. 1a, $C_{35}H_y$, $C_{35}H_{y+1}$, $C_{35}H_{y+2}$, $C_{36}H_y$, $C_{36}H_{y+1}$ and $C_{36}H_{y+2}$, become $C_{35}D_y$, $C_{35}D_{y+1}$, $C_{35}D_{y+2}$, $C_{36}D_y$, $C_{36}D_{y+1}$ and $C_{36}D_{y+2}$ in Fig. 1b. The relative intensities of the individual ion peaks were varied to obtain a good match between the calculated total profiles (heavy lines) and the experimental profiles (symbols). The deduced intensity patterns are not identical for the two flames (perhaps due to somewhat different flame conditions) yet the spectra both are dominated by $C_{35}H_y$, $C_{35}H_{y+2}$, $C_{36}H_y$, $C_{36}H_{y+2}$, and the corresponding deuterated ions, with intensities of y greater than y+2 for C_{35} and y less than y+2 for C_{36}. Small contributions from ions with H_{y+1} may be indicated, but we feel unjustified on the basis of the poor spectral resolution to accept their presence as confirmed. For all carbon numbers above C_{13}, the deuterated peaks were considerably broader than the protonated peaks.

This analysis indicates that the peaks include at least two different ionic species which differ by two hydrogen atoms, corresponding to 2 amu and 4 amu in the C_2H_2 and C_2D_2 flames, respectively. Oxygenated species cannot be ruled out as also being present, for if $C_{x-1}H_{y-2}O$ (with the same mass as C_xH_{y+2}) is deuterated, the new ion will have the same mass as C_xD_y. This would only show up as a shift of relative intensity to this first peak coincident with C_xD_y. Observation of this was difficult since the intensity pattern in the protonated peaks could not be discerned directly.

The simulations presented in Fig. 1 also show that the C_{35} and C_{36} pairs differ only by one carbon atom and have the same hydrogen contents. Because of the switching of the dominant ion ($C_{35}H_y$ and $C_{36}H_{y+2}$) the apparent C_{35} to C_{36} mass difference for the overall peaks appear to be larger than 12 amu. If the alternate peaks dominated (e.g., $C_{36}H_{y+2}$ and $C_{37}H_y$ dominating) a value less than 12 amu would be apparent. This "switching" phenomenon was observed in the protonated spectrum and further supports the contribution of two ion masses to the apparent ion peaks, and it provides a rationale by which to judge which ion peaks exhibit a change in hydrogen content. Using an "aufbau" approach we were able to follow the chemical composition change from the well known $C_{13}H_9^+$ ion to the high mass limit of the spectrometer. From the composition of the ions, the masses were determined and were found to be as much as 5-10 amu lower than would be determined using a simple linear extrapolation of the low mass data to the ≥ 500 amu range. The polynomials used to correct the initially deduced masses, M_0, were, for the mass range to 165 amu:

$$M_{true} = -2.9983 + 1.1149M_0 - 9.2304 \times 10^{-4} M_0^2 + 2.0143 \times 10^{-6}M_0^3$$

and for the mass range above 165 amu:

$$M_{true} = 6.1210 + 0.9594M_0 + 6.0489 \times 10^{-5}M_0^2 - 9.5347 \times 10^{-8}M_0^3$$

Our best estimates for the large ion identities are given in Table II. Suggested structures for all of these ions are presented in Table III. Alternate structures are possible for some of the ions but given the C/H ratio and the rules for organic chemistry there is not as much freedom in choosing a structure as one might initially suppose. The largest ion observed, $C_{45}H_{19}$, mass 559, is still small compared to the smallest soot particle observed, The molecular ions in Table III would most probably be flat plates with diameters up to about 1.0 nm for mass 559 compared with the 1.5 nm diameter of the smallest observed soot particle.[3]

C. MASS SPECTRA

We have obtained ion spectra for acetylene-oxygen flames at 2.7 kPa, 50 cm/s unburned gas flow for Ø= 1.0, 1.5, 2.0, 2.25, 2.5, 2.6, 2.7, 2.8, 2.9, and 3.0. This spans the range from nonsooting to well into the sooting range; the soot threshold for this flame is at Ø = 2.4. Some of the results are presented in Fig. 2 for a flame at Ø= 2.5. The other results will not be

reported until we have calibrated the system so that the mass spectrometer ion current can be corrected to ion concentration. This should be done in the next reporting period. Interpretation of the data will also wait for completion of the calibration.

In the above spectra all of the ions contain an odd number of hydrogens. This is contrasted with the predictions of Stein[18] for this flame. Stein argues from thermodynamics and kinetics that the equilibrium:

$$BPAH\text{-}H^+ \rightleftharpoons BPAH^{\cdot +} + H^{\cdot}, \qquad (1)$$

where BPAH-H$^+$ is a protonated benzenoid polyaromatic hydrocarbon (many of the species in the above sequence) and BPAH$^{\cdot +}$ is an ionized benzenoid polyaromatic, is always to the right-hand side in this flame in the temperature range above 1500-1800 K. He accounts for our observations by arguing that the ions in a volume of the flame cooled by the sampling probe are cooled below ~1500 K so that BPAH$^{\cdot +}$ is irreversibly converted to BPAH-H$^+$ in several microseconds. Assuming a rate constant of 10^{-10} cm^3 molecule^{-1} s^{-1} for the protonation reaction he deduces a half-life of 3×10^{-6} s. While we do not know the rate of cooling in our particular nozzles, Hayhurst and Telford[19] in an extensive analysis for similar nozzles estimate a flow time through the nozzle of about 5×10^{-7} s. It thus seems reasonable to conclude that the ions we observe are the actual ions in the flame and that the equilibrium discussed by Stein does not play a major role in shuffling the ions. Further note that the observed ions with odd numbers of hydrogen atoms are just what is predicted assuming $C_3H_3^+$ as the initial ion.

D. REACTION HEATING OF SOOT PARTICLES

In the ionic mechanism of soot formation it is assumed that the large ions and very small charged soot particles are formed by the growth of smaller ions by the addition of small neutral species, such as acetylene. Others attempt to explain the presence of these ions and small charged particles by other mechanisms. Homann has proposed[11] that as the incipient soot particles grow, the exothermic growth reactions deposit energy in the particles more rapidly than they can dissipate the energy. The particle temperature thus exceeds the gas temperature so the particles are thermally ionized. Homann has not developed a quantitative description of the phenomena[20] ; it is incumbent upon us to analyze this alternate mechanism.

We thus have made quantitative estimates of the amount of reactive heating expected for growing species in a ϕ = 3.0, 2.67 kPa C_2H_2/O_2 premixed flame (50 cm s^{-1} unburned gas velocity). The model selected is similar to that used by Millikan[21] to estimate particle temperatures. We first describe the model and quantitative estimates of the various input parameters, and then discuss the implications on particle heating.

Growth of species from molecular size (150 amu) to particle size (10^5 amu) is considered. P_n, designates a particle which has undergone n reactive

collisions. The particle is heated in the growth reaction with species G,

$$P_{n-1}\ (T_0) \ + \ G \xrightarrow{k_G(n)} P_n \ \ T_0 + \frac{q_G}{C_n}$$

where $k_G(n)$ is the reaction rate constant for the process creating P_n. The initial temperature of the precursor, P_{n-1}, is T_0, and the entire exothermicity, q_G, of the reaction is assumed to heat particle P_n of heat capacity, C_n.

Particle cooling occurs either radiatively or by collisions with the flame species, M, as described by the process:

$$P_n(T_i) \ + \ M \xrightarrow{k_M(n)} P_n \left[T_i - \frac{q_M}{C_n} \right] \ + \ M$$

where q_M is the energy transferred to the bath gas, and $k_M(n)$ represents the collision rate constant of M with P_n.

Several properties of the low pressure C_2H_2/O_2 flames lead to simplification of the model. Relative to the range of particle sizes considered here (10 nm diam), the gas mean free path is very large (typically on the order of 10 μm) compared to the particle diameter so molecular heat transfer processes dominate. For simplicity we neglect radiative cooling of the hot particles so that an upper limit to particle heating is obtained.

The reactive heating rate is approximated as the enthalpy of the growth reaction, ΔH_G, times the rate of reactive collisions of the growth species G with the particle: $\Delta H_G\ k_G[G]$. The rate constant, k_G, can be written as the product $f_G Z_G[G]$ where Z_G is the collision rate of G with the particle and f_G is the fraction of collisions which are reactive. Similarly, the rate of heat transfer to the flame gases is approximated as $q_M Z_M[M]$ where q_M is the heat transfer per collision between the particle and M, and Z_M is the collision rate. q_M is given by:

$$q_M \ = \ \alpha \ C_M \ \Delta T \qquad (1)$$

where α is the accommodation coefficient for energy transfer from the particle to M, C_M is the heat capacity of M, and ΔT represents temperature difference between the particle and the flame, $T_p - T_f$.

The competition of these two processes will result in particle heating to a steady-state temperature determined by the condition:

$$\Delta H_G f_G Z_G[G] \ + \ q_M Z_M[M] \ = \ 0.$$

The particle temperature is then given by:

$$T_p(\infty) = T_F - \frac{\Delta H_G f_G Z_G [G]}{\alpha C_M Z_M [M]} \quad (2)$$

$T_p(\infty)$ represents the "steady-state" temperature of the particles; the particle "temperature" will initially be a function of time.

We first consider the steady-state particle temperatures for various "particle" sizes from molecular size (150 amu) to 10^5 amu, corresponding to a spherical particle diameter, d_p, of 6 nm (density = 1.5). It will be shown that to a first approximation, $T_p(\infty)$ is independent of the particle size. Thus the particle temperature can be considered independent of its growth history once "steady-state" is reached. The denominator of the right hand term of Eq. (2) is:

$$\alpha c_M Z_M [M] = \sum_i \alpha_i C_i Z_i X_i [M] \quad (3)$$

where the sum is taken over the major flame components with mole fractions X_i, and [M] is the total gas concentration. For the $\emptyset$ = 3.0 flame, the major species are CO, H_2 and C_2H_2 in approximate ratio[5,9] of 6:3:1 and [M] = 1×10^{17} molecules cm^{-3} at 2000 K and 2.7 kPa. The collision number Z_i from kinetic theory is:

$$Z_i = \pi \left[\frac{d_p + d_i}{2}\right]^2 \left[\frac{8kT}{\pi \mu_i}\right]^{0.5} \quad (4)$$

where μ_i is the reduced mass of the particle/reactant pair. For large particles this smoothly goes over into the rate of molecules i colliding with the surface of a spherical particle,

$$Z_i = \frac{\pi d_p^2}{4} \left[\frac{8kT}{\pi m_i}\right]^{0.5} \quad (5)$$

Even for a particle of mass 150, use of m_i rather than μ_i results in less than 10% error in the collision number, and the variation in d_i for H_2, CO, and C_2H_2 (0.2-0.4 nm)[22] is small relative to d_p (~ 1 nm). Assuming α to be independent of the gas, we calculate an effective value for Eq. (3) at 2000 K in terms of the CO diameter, d_{CO}, which will be essentially valid for all particle sizes. The heat capacities used were estimated to be (kJ K^{-1} $mole^{-1}$) 26, 29, and 75 for H_2, CO, and C_2H_2, respectively.[23] Likewise the reaction collision number Z_ϕ can be simplified. Equation (2) is now (employing m_ϕ ~ 26 amu for acetylene, the only real growth candidate)[24-26]

$$T_p \approx T_F - \frac{19\ \Delta H_G\ f_G X_G (d_p + d_G)^2 [M]}{\alpha (d_p + d_{CO})^2\ [M]} \qquad (6)$$

where ΔH_G is in kJ mole^{-1} and the diameters are in angstroms. Assuming $d_G \approx d_{CO} \ll d_p$, or when d_p is very large, the size dependence (except any hidden in α) drops out and

$$T_p \approx T_F - \frac{19(\Delta H_G / \text{kJ mole}^{-1})\ f_G X_G}{\alpha} \qquad (7)$$

This equation holds equally well for molecules and particles from 150-10^5 amu in a $\phi = 3.0$ flame. Now, in order to evaluate T_p, we need to estimate the heat of reaction which we have assumed involves the major hydrocarbon species, C_2H_2. We note that mass spectrometric measurements in low pressure C_2H_2/O_2 flames have shown that the next most abundant hydrocarbon species, C_4H_2, is an order of magnitude lower in concentration.[5,9]

Mature soot particles show considerable graphitic nature while small, young particles have higher H/C ratios which decrease as the particle grows. We estimate the exothermicity of the growth reactions by two overall processes.

$$C_2H_2 \rightarrow 2C(s) + H_2 \qquad \Delta H_{298} = -227 \text{ kJ mole}^{-1}$$

$$1/4C_6H_6 + C_2H_2 \rightarrow 1/4C_{14}H_{10} + 1/2H_2 \qquad \Delta H_{298} = -178 \text{ kJ mole}^{-1}$$

Using available heat capacity data,[23,27] at 2000 K, the processes have exothermicities of about 210 and 165 kJ mole^{-1}, respectively. Thus Eq. (7) becomes:

$$T_p \leq T_F + \frac{400 f_G}{\alpha} \qquad (8)$$

for the more exothermic process.

The coefficients, f_G and α, remain the major uncertainties as Millikan found.[21]

Energy transfer in reacting molecular systems has been investigated both for thermal and chemically activated systems. The efficiency of energy transfer is expressed in terms of an average energy step based on a model of energy

transfer probability. A number of investigations have shown that the mean energy transferred per collision decreases with increasing temperature.[28-30] Particularly apropos to the accommodation coefficient α for present considerations are experiments by Barker and coworkers[29,31] on vibrational energy transfer from highly excited ground electronic state azulene produced in internal conversion of the laser excited molecule. This mimics the exothermic growth process in that the vibrational temperature of the large molecule is much higher than that of the bath gas. Using different wavelengths for excitation, the dependence of the transferred energy on the azulene energy content was probed.[31] The average collisional energy transfer to CO was about 375 cm^{-1} for azulene excitation of 30,600 cm^{-1}, and it was 150 cm^{-1} for 17,500 cm^{-1} excitation. These values correspond to $\alpha \approx 0.2$ and 0.1 for CO in the high and low energy excitations, respectively. The corresponding values (energy transferred and α) for H_2 (about the same heat capacity as CO) were roughly half of these. Barker and Golden [29] found roughly a $T^{-0.5}$ dependence for the average energy transferred to the diatomic N_2 in the azulene system. In the range 300-525 K it was about 295 cm^{-1} at room temperature, and it dropped to 180 cm^{-1} from 400 to 525 K in good agreement with the observations of Brown et al.[30] for N_2 in ethyl acetate from 300-800 K. Also, Heymann et al.[32] found the average energy transferred to CO from cycloheptatriene to exhibit a roughly $T^{-0.5}$ dependence while other monatomic and diatomics exhibited somewhat lower temperature dependencies. Considering the major post flame component CO, we correct the conservative $\alpha = 0.1$ to flame temperatures by scaling by the inverse square root of the temperature which gives $\alpha \approx 0.04$.

Gas-surface accommodation coefficients, f_ϵ, are generally fairly high at room temperature (0.3-1) and also have been observed to decrease with increasing temperatures. In a study of gas-surface single-collision energy transfer, Rabinovitch and coworkers[33] found a vibrational accommodation coefficient of 0.2 for cyclobutene on quartz at 975 K. We assume that α for the particles is at least as large as the molecular value of 0.04 estimated above.

The particle growth rate is obtained from the electron microscopic studies by Howard and coworkers.[6] From their results they calculated surface growth rates for soot particles in the "standard" acetylene-oxygen flame (P = 2.7 kPa, u = 50 cm/s) below about 2.5 μm/s. This corresponds with an estimated value of f_ϵ on the order of 0.01 for C_2H_2 as the growth species. This compares with a maximum value of $f_\epsilon = 0.001$ (for C_2H_2) from the atmospheric pressure flame measurements of Harris and Weiner.[24-26]

Substituting $\alpha = 0.04$ and $f_\epsilon = 0.01$ in Eq. (8) gives a temperature for the particle 100 K greater than the gas temperature. If we increase the measured gas temperature by 100 K and calculate the total ion concentration using Saha's equation the results reported in Fig. 3. are obtained. The small increase in equilibrium concentration of charged particles still gives a theoretical concentration below the experimental value. The decrease in the measured value with distance is consistent with the picture that the ions are formed in the flame front and then disappear by ion-electron recombination. At further distances from the burner the measured and calculated charged particle concentrations may agree because when the particles become larger

thermal equilibrium ionization prevails. This is completely different from the ionization we are concerned about in the earlier part of the flame; unfortunately the two parts of the flame are often confused.

The results reported in Fig. 3 do not support Homann's proposal.[11] We are not as confident as we would like to be however with the values of α and f_e so have held up publication until we can find more reliable values.

III. PUBLICATIONS

The following papers were published during this report period:

1. "Ionization and Soot Formation in Premixed Flames," D.G. Keil, R.J. Gill, D.B. Olson, and H.F. Calcote, Twentieth Symposium (International) on Combustion (The Combustion Institute, Pittsburgh, 1985) p. 1129.

2. "The Effect of Temperature on Soot Formation in Premixed Flames," D.B. Olson and S. Madronich, Combust. Flame 60, 203 (1985).

The following manuscript is in preparation:

1. "Langmuir and Thermocouple Probe Measurements in Flames," D.G. Keil, R.J. Gill, D.B. Olson, and H.F. Calcote..

IV. PERSONNEL

In addition to the authors the following personnel made significant contributions to this program:

D.B. Olson, Physical Chemist
H. Rothschild, Librarian, Technical Editor
(Ms. Rothschild also assisted with data reduction.)
E.L. Stokes, Technical Typist

V. TECHNICAL INTERACTIONS

Technical interactions with the scientific community have taken several forms; the most important are presentations at scientific meetings, seminars and workshops. Proposal and manuscript review has also played an important role during this report period. Olson and Calcote visited Dr. Charles Martel at Wright Field to discuss our work, especially the effect of fuel molecular structure on jet engine performance. The following people visited AeroChem during this contract to discuss the mechanism of soot formation at a workshop sponsored by Army Research Office:

T. Brabbs and E. Lezberg (NASA/Lewis Research Center)
J. Eyler (University of Florida
W. Flower (Sandia National Laboratories)
M. Frenklach and T. Lester (Louisiana State University)
I. Glassman, A. Gomez, and G. Sidebotham (Princeton University)
S. Harris (General Motors Research Laboratories)
R. D. Kern (University of New Orleans)
W. G. Mallard and R. Santoro (National Bureau of Standards)
D. Mann (U.S. Army Research Office)
J. Tishkoff (Air Force Office of Scientific Research)

The following presentations were made:

1. "Soot Formation in Flames" Presented by H.F. Calcote to six separate groups on a "People To People" tour through China in which Calcote was the Delegation Leader, 9-30 October 1984.

2. "The Effect of Temperature on Soot Formation in Premixed Flames" D.B. Olson, Eastern States Section: The Combustion Institute, Fall Technical Meeting, Clearwater, FL, December 1984.

3. "The Role of Ions and Charged Particles in Soot Formation" H. F. Calcote, Seminar Rutgers University, Engineering and Aerospace Dept. 10 April 1985

4. "An Ionic Mechanism of Soot Formation in Flames" Calcote, invited presentation at the Particle Emission Technology Meeting", Naval Post graduate School, Monterey, CA, 16-18 April 1985

VI. INVENTIONS AND PATENT DISCLOSURES

There are no inventions or patent disclosures to report during this reporting period.

VII. REFERENCES

1. Calcote, H.F., "Ionic Mechanism of Soot Formation," in Soot in Combustion Systems and Its Toxic Properties, J. Lahaye and G. Prado, Eds. (Plenum Press, New York, 1983) p. 197.

2. Calcote, H.F. "Mechanism of Soot Nucleation in Flames - A Critical Review," Combust. Flame 42, 215 (1981).

3. Howard, J.B., Wersborg, B.L., and Williams, G.C., "Coagulation of Carbon Particles in Premixed Flames," Faraday Soc. Symp. 7, 109 (1973).

4. Wersborg, B.L., Yeung, A.C., and Howard, J.B., "Concentration and Mass Distribution of Charged Species in Sooting Flames," Fifteenth Symposium (International) on Combustion (The Combustion Institute, Pittsburgh, 1975) p. 1439.

5. Bittner, J.D. and Howard, J.B., "Pre-Particle Chemistry in Soot Formation," in Particulate Carbon: Formation During Combustion, D.C. Siegla and G.W. Smith, Eds. (Plenum Press, New York, 1981) p. 109.

6. Wersborg, B.L., Howard, J.B., and Williams, G.C., "Physical Mechanisms in Carbon Formation in Flames," Fourteenth Symposium (International) on Combustion (The Combustion Institute, Pittsburgh, 1973) p. 929.

7. Michaud, P., Delfau, J.L., and Barassin, A., "The Positive Ion Chemistry in the Post-Combustion Zone of Sooting Premixed Acetylene Low Pressure Flat Flames," Eighteenth Symposium (International) on Combustion (The Combustion Institute, Pittsburgh, 1981) p. 443.

8. Delfau, J.L., Michaud, P., and Barassin, A., "Formation of Small and Large Positive Ions in Rich and Sooting Low-Pressure Ethylene and Acetylene Premixed Flames," Combust. Sci. Tech. 20, 165 (1979).

9. Delfau, J.L. and Vovelle, C., "Mechanism of Soot Formation in Premixed C_2H_2/O_2 Flames," Combust. Sci. Tech. 41, 1 (1984).

10. Homann, K.H., "Formation of Large Molecules, Particulates and Ions in Premixed Hydrocarbon Flames; Progress and Unresolved Questions," Twentieth Symposium (International) on Combustion (The Combustion Institute, Pittsburgh, 1985) p. 857.

11. Homann, K.H., "Charged Particles in Sooting Flames I. Determination of Mass Distributions and Number Densities in C_2H_2-O_2 Flames," Ber. Bunsenges. Phys. Chem. 83, 738 (1979).

12. Homann, K.H., Strofer, E., and Wolf, H., "Growth of Electrically Charged Soot Particles in Flames," Combustion Problems in Turbine Engines, AGARD Conference Proceedings No. 353, January 1984, p. 19-1. (1984).

13. Homann, K.H. and Schweinfurth, H., "Kinetics and Mechanism of Hydrocarbon Formation in the System $C_2H_2/O/H$," Ber. Bunsenges. Phys. Chem. 85, 569 (1981).

14. Howard, J.B., MIT, Personal communication.

15. Olson, D.B. and Calcote, H.F., "Ions in Fuel-Rich and Sooting Acetylene and Benzene Flames," Eighteenth Symposium (International) on Combustion (The Combustion Institute, Pittsburgh, 1981) p. 453.

16. Keil, D.G., Gill, R.J., Olson, D.B., and Calcote, H.F., "Ion Concentrations in Premixed Acetylene-Oxygen Flames Near the Soot Threshold," in Chemistry of Combustion Processes, T.M. Sloane, Ed., ACS Symposium Series 249 (American Chemical Society, Washington, DC, 1984) p. 33.

17. Keil, D.G., Gill, R.J., Olson, D.B. and Calcote, H.F., "Ionization and Soot Formation in Premixed Flames," Twentieth Symposium (International) on Combustion (The Combustion Institute, Pittsburgh, 1985) p. 1129.

18. Stein, S.E., "Structure and Equilibria of Polyaromatic Flame Ions," Combust. Flame 51, 357 (1983).

19. Hayhurst, A.N. and Telford, N.R., "The Occurrence of Chemical Reactions in Supersonic Expansions of a Gas into a Vacuum and Its Relation to Mass Spectrometric Sampling," Proc. Roy. Soc. Lond. A 322, 483 (1971).

20. Homann, K.H., Personal communication, August 1984.

21. Millikan, R.C., "Sizes, Optical Properties, and Temperatures of Soot Particles," in Temperature; Its Measurement and Control in Science and Industry, Vol. 3, C.M. Herzfeld, Ed. (Reinhold Publishing Corp., New York, 1962) p. 497.

22. Hirschfelder, J.O., Curtiss, C.F., and Bird, R.B., Molecular Theory of Gases and Liquids, (Wiley, New York, 1954).

23. Benson, S.W., Thermochemical Kinetics, 2nd Ed. (Wiley, New York, 1976).

24. Harris, S.J. and Weiner, A.M., "Surface Growth of Soot Particles in Premixed Ethylene/Air Flames," Combust. Sci. Tech. 31, 155 (1983).

25. Harris, S.J. and Weiner, A.M., "Soot Particle Growth in Premixed Toluene/Ethylene Flames," Combust. Sci. Tech. 38, 75 (1984).

26. Harris, S.J. and Weiner, A.M., "Chemical Kinetics of Soot Particle Growth," Ann. Rev. Phys. Chem. 36, 31 (1985).

27. Handbook of Physics and Chemistry, 61st Ed. (CRC Press, Boca Raton, 1980).

28. Krongauz, V.V. and Rabinovitch, B.S., "Competitive Collisional Activation in Vibrational Energy Transfer with Cyclopropane-$1t_1$-$2,2d_2$. A Three-Channel System," Chem. Phys. 67, 201 (1982).

29. Barker, J.R. and Golden, R.E., "Temperature-Dependent Energy Transfer: Direct Experiments Using Azulene," J. Phys. Chem. 88, 1012 (1984).

30. Brown, T.C., Taylor, J.A., King, K.D., and Gilbert, R.G., "Temperature Dependence of Collisional Energy Transfer in Ethyle Acetate," J. Phys. Chem. 87, 5214 (1983).

31. Rossi, M.J., Pladziewicz, J.R., and Barker, J.R., "Energy-Dependent Energy Transfer: Deactivation of Azulene (S_0, $E_{v;s}$) by 17 Collider Gases," J. Chem. Phys. 78, 6695 (1983).

32. Heymann, M., Hippler, H., and Troe, J., "Collisional Deactivation of Vibrationally Highly Excited Polyatomic Molecules. IV. Temperature Dependence of (ΔE)," J. Chem. Phys. 80, 1853 (1984).

33. Kelley, D.F., Kasai, T., and Rabinovitch, B.S., "Single-Collision Gas-Surface Vibrational Energy Transfer in a Reacting System," J. Phys. Chem. 85, 1100 (1981).

TABLE I

WHY I BELIEVE IN THE IONIC MECHANISM OF SOOT FORMATION IN FLAMES

1. Fuel effects: the propensity to form soot correlates with the tendency of the fuel to produce ions.

2. Chemical additive effects: the explanation of some additive effects is contingent upon an ionic mechanism of incipient soot formation - not to be confused with ionic additive effects on soot agglomeration.

3. Soot formation is a nonequilibrium process at the critical equivalence ratio for soot formation; it thus needs a nonequilibrium process to drive it--chemi-ionization is a nonequilibrium process.

4. Ion-molecule reactions to explain the phenomena are easy to prescribe, no ad hoc assumptions are required--compare the problems with free radical reactions. For example:

    a. The ions required in the mechanism have been observed in flames.

    b. Ion-molecule reactions are fast.

    c. Isomerization of ions is very fast; explains the transition from a linear structure to a cyclic structure - a major problem with free radical mechanisms.

5. The concentration and rates of ion formation seem to be adequate to account for the appearance of soot--there may be some questions here because of the limited number of tests and the quality of the soot concentration data.

6. Dramatic changes occur in the ions at the soot threshold, consistent with what would be expected for an ionic mechanism.

7. Variation in ion composition and location of ion profiles with respect to soot formation is consistent with an ionic mechanism of formation of incipient soot.

TABLE II

ION IDENTITIES OF MAJOR HEAVY IONS OBSERVED IN RICH C_2H_2/O_2 FLAMES

$C_{18}H_{11,13}^+$	$C_{32}H_{15,17}^+$
$C_{19}H_{11,13}^+$	$C_{33}H_{15,17}^+$
$C_{20}H_{11,13}^+$	$C_{34}H_{15,17}^+$
$C_{21}H_{11,13}^+$	$C_{35}H_{15,17}^+$
$C_{22}H_{13,15}^+$	$C_{36}H_{15,17}^+$
$C_{23}H_{13,15}^+$	$C_{37}H_{15,17}^+$
$C_{24}H_{13,15}^+$	$C_{38}H_{15,17}^+$
$C_{25}H_{13,15}^+$	$C_{39}H_{15,17}^+$
$C_{26}H_{13,15}^+$	$C_{40}H_{17,19}^+$
$C_{27}H_{13,15}^+$	$C_{41}H_{17,19}^+$
$C_{28}H_{13,15}^+$	$C_{42}H_{17,19}^+$
$C_{29}H_{13,15}^+$	$C_{43}H_{17,19}^+$
$C_{30}H_{15,17}^+$	$C_{44}H_{17,19}^+$
$C_{31}H_{15,17}^+$	$C_{45}H_{17,19}^+$

TABLE III

SUGGESTED STRUCTURES OF OBSERVED FLAME IONS

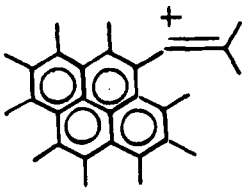

$C_{18}H_{11}^{+}$ (227)

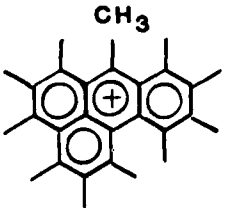

$C_{18}H_{13}^{+}$ (229)

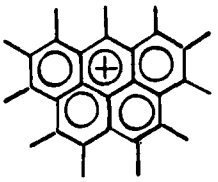

$C_{19}H_{11}^{+}$ (239)

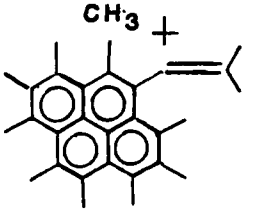

$C_{19}H_{13}^{+}$ (241)

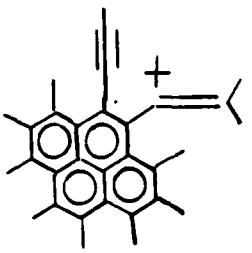

$C_{20}H_{11}^{+}$ (253)

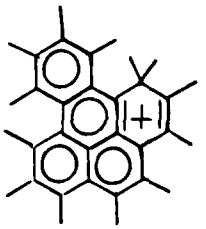

$C_{20}H_{13}^{+}$ (255)

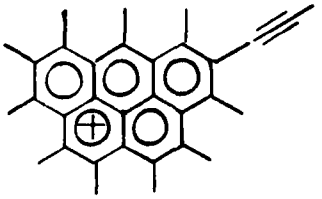

$C_{21}H_{11}^{+}$ (265)

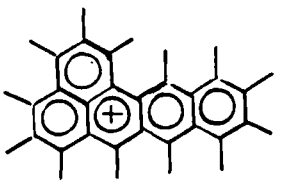

$C_{21}H_{13}^{+}$ (267)

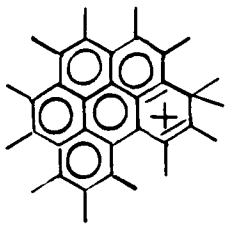

$C_{22}H_{13}^{+}$(277)

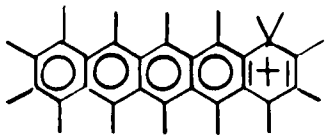

$C_{22}H_{15}^{+}$ (279)

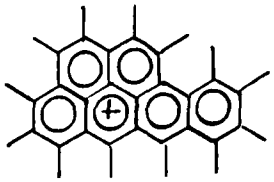

$C_{23}H_{13}^{+}$ (289)

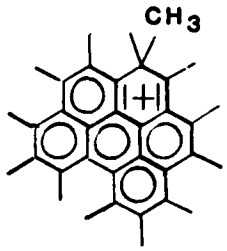

$C_{23}H_{15}^{+}$ (291)

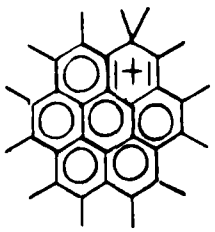

$C_{24}H_{13}^{+}$ (301)

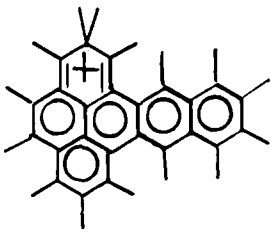

$C_{24}H_{15}^{+}$ (303)

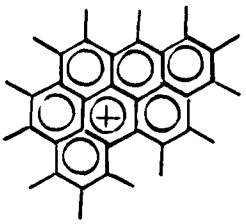

$C_{25}H_{13}^{+}$ (313)

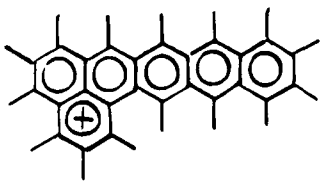

$C_{25}H_{15}^{+}$ (315)

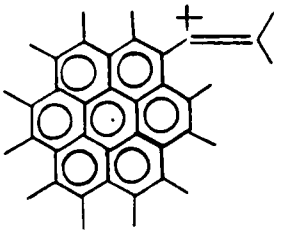

$C_{26}H_{13}^{+}$ (325)

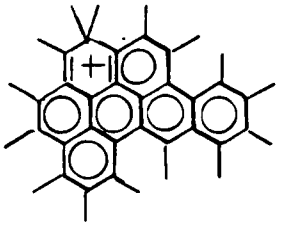

$C_{26}H_{15}^{+}$ (327)

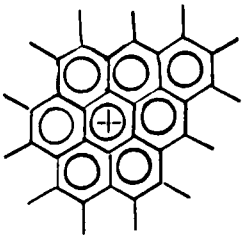

$C_{27}H_{13}^{+}$ (337)

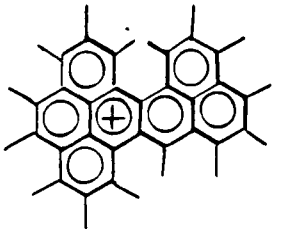

$C_{27}H_{15}^{+}$ (339)

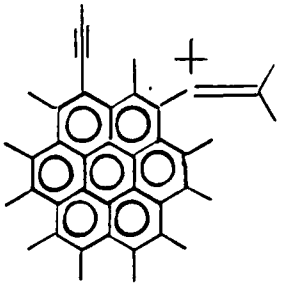

$C_{28}H_{13}^{+}$ (349)

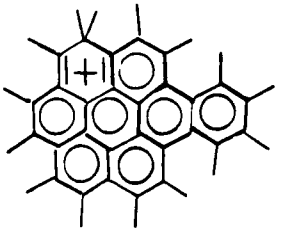

$C_{28}H_{15}^{+}$ (351)

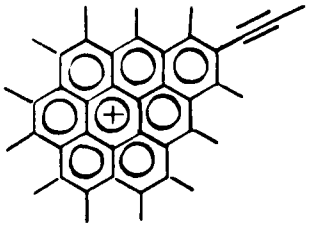

$C_{29}H_{13}^{+}$ (361)

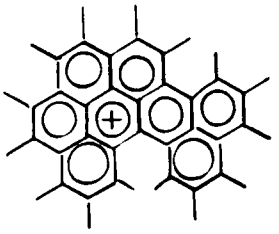

$C_{29}H_{15}^{+}$ (363)

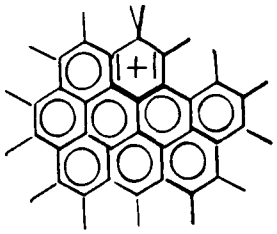

$C_{30}H_{15}^{+}$ (375)

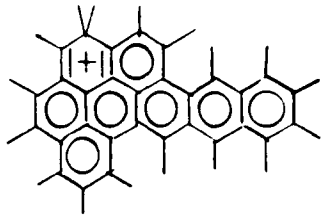

$C_{30}H_{17}^{+}$ (377)

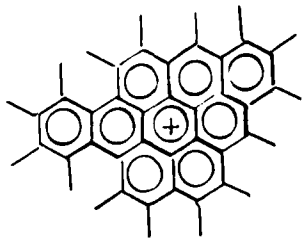

$C_{31}H_{15}^{+}$ (387)

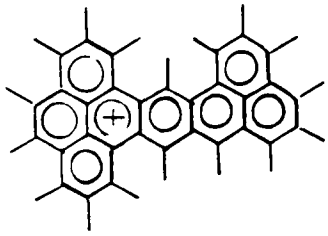

$C_{31}H_{17}^{+}$ (389)

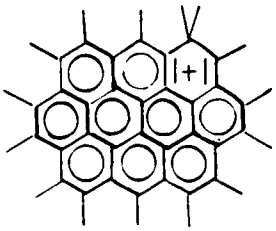

$C_{32}H_{15}^{+}$ (399)

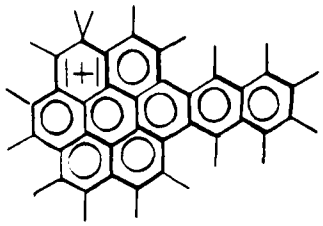

$C_{32}H_{17}^{+}$ (401)

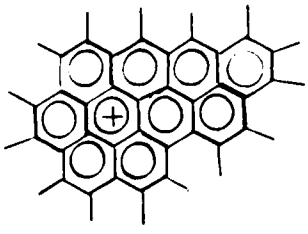

$C_{33}H_{15}^{+}$ (411)

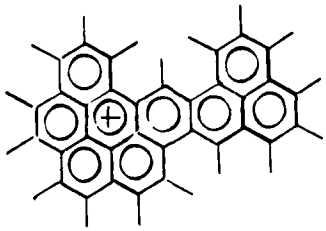

$C_{33}H_{17}^{+}$ (413)

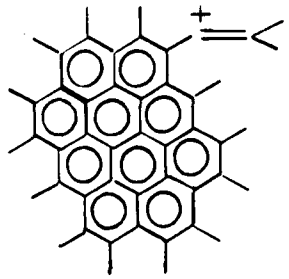

$C_{34}H_{15}^{+}$ (423)

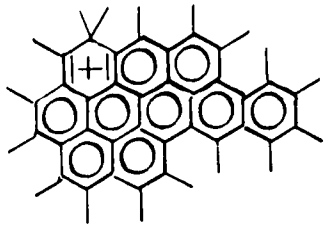

$C_{34}H_{17}^{+}$ (425)

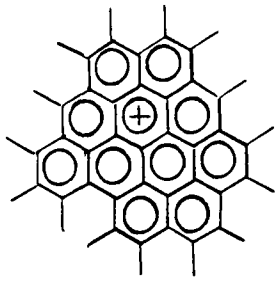

$C_{35}H_{15}^{+}$ (435)

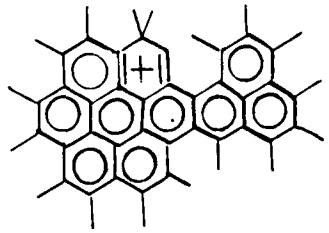

$C_{35}H_{17}^{+}$ (437)

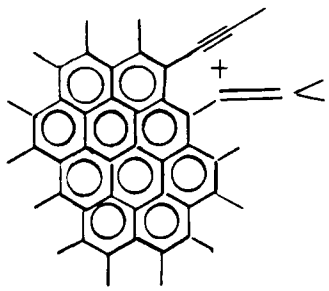

$C_{36}H_{15}^{+}$ (447)

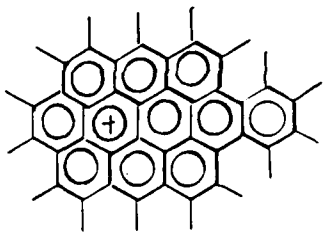

$C_{36}H_{17}^{+}$ (449)

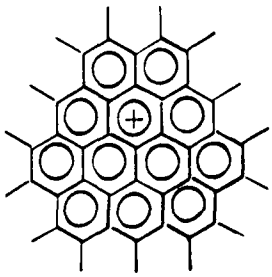

$C_{37}H_{15}^{+}$ (459)

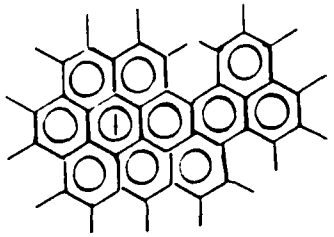

$C_{37}H_{17}^{+}$ (461)

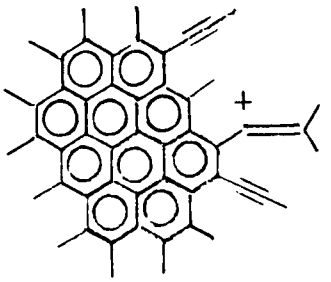

$C_{38}H_{15}^{+}$ (471)

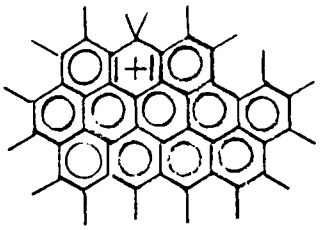

$C_{38}H_{17}^{+}$ (473)

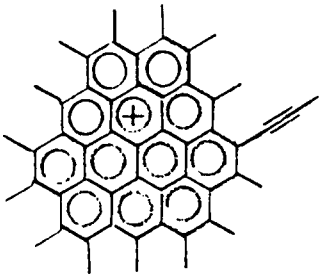

$C_{39}H_{15}^{+}$ (483)

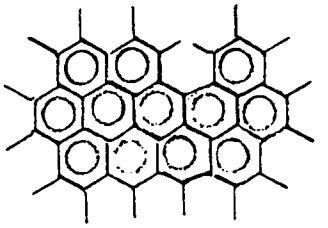

$C_{39}H_{17}^{+}$ (485)

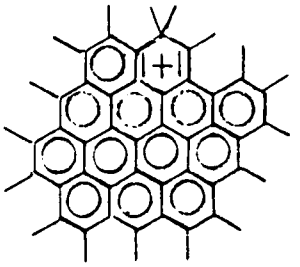

$C_{40}H_{17}^{+}$ (497)

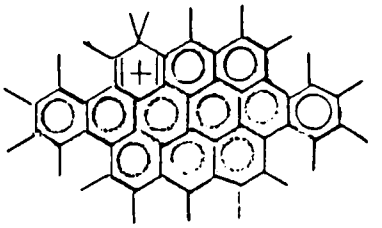

$C_{40}H_{19}^{+}$ (499)

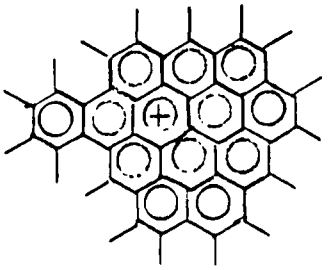

$C_{41}H_{17}^{+}$ (509)

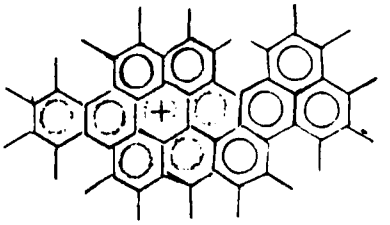

$C_{41}H_{19}^{+}$ (511)

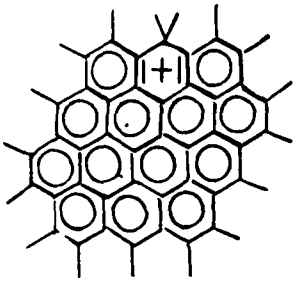

$C_{42}H_{17}^{+}$ (521)

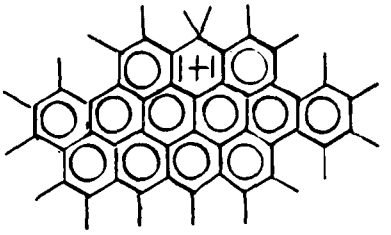

$C_{42}H_{19}^{+}$ (523)

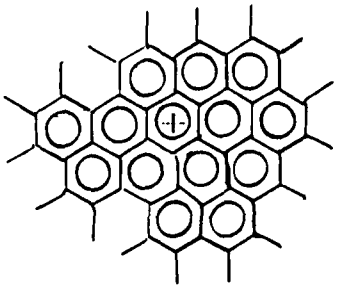

$C_{43}H_{17}^{+}$ (533)

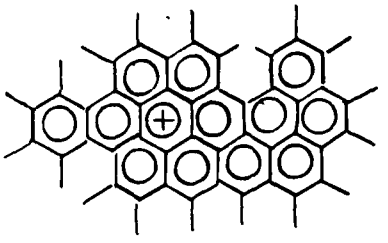

$C_{43}H_{19}^{+}$ (535)

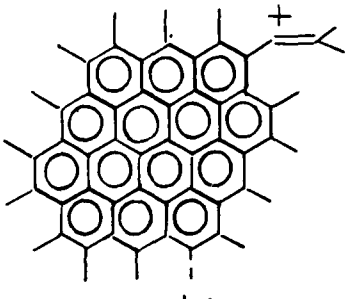

$C_{44}H_{17}^{+}$ (545)

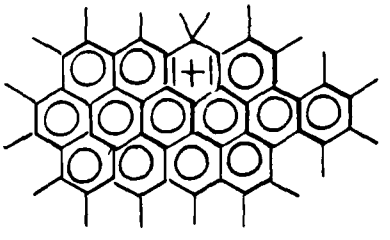

$C_{44}H_{19}^{+}$ (547)

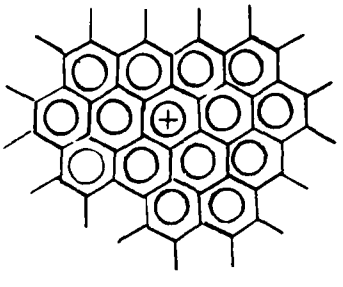

$C_{45}H_{17}^{+}$ (557)

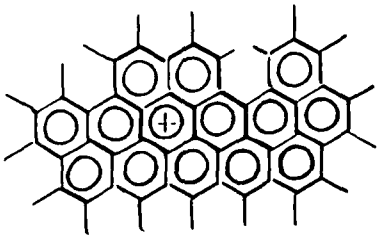

$C_{45}H_{19}^{+}$ (559)

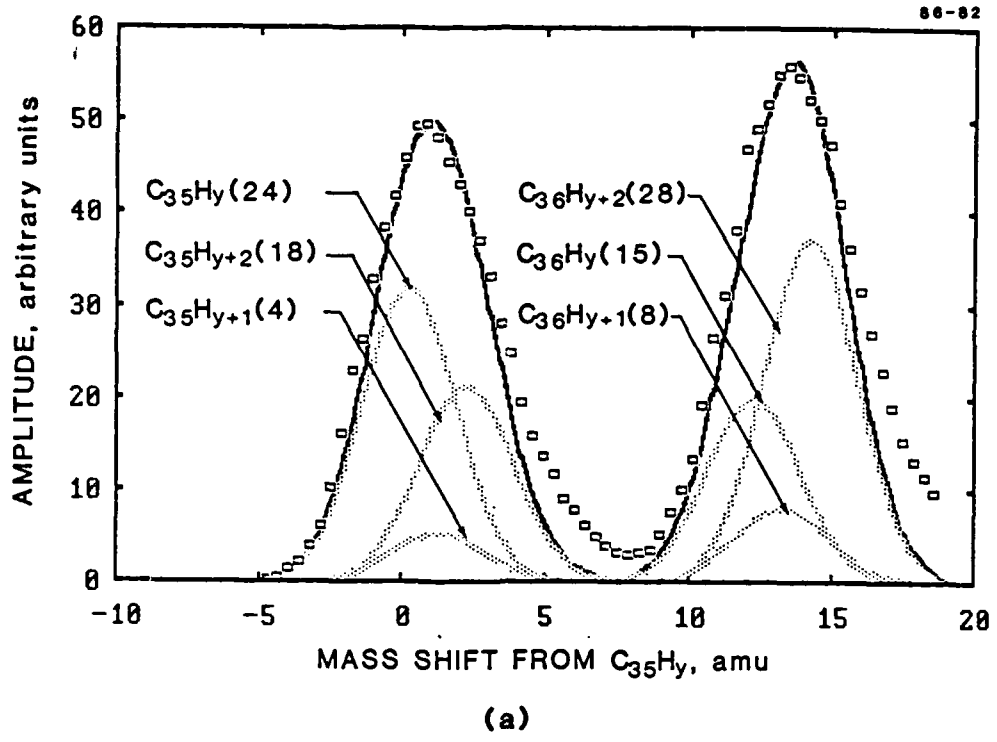

(a)

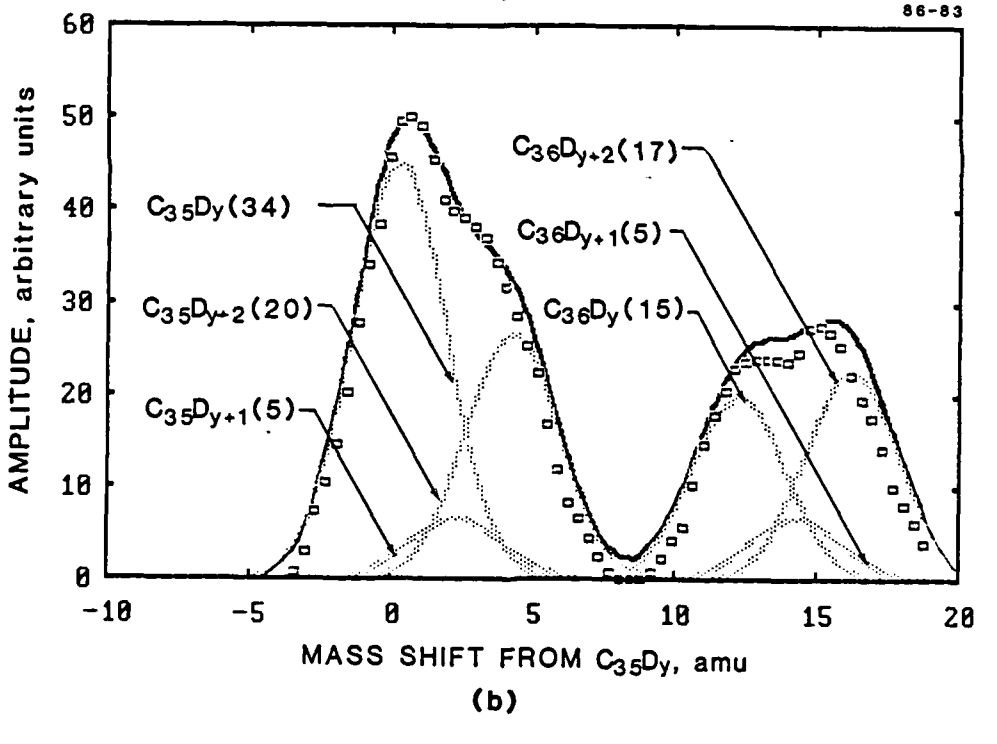

(b)

FIGURE 1 COMPARISONS OF CALCULATED AND EXPERIMENTAL ION PEAKS. C_2H_2 AND C_2D_2 FLAMES

Sparse lines - simulated peaks for species indicated, (relative intensities in parentheses). Heavy lines - sum of calculated individual peaks. □ - experimental profiles (see text).

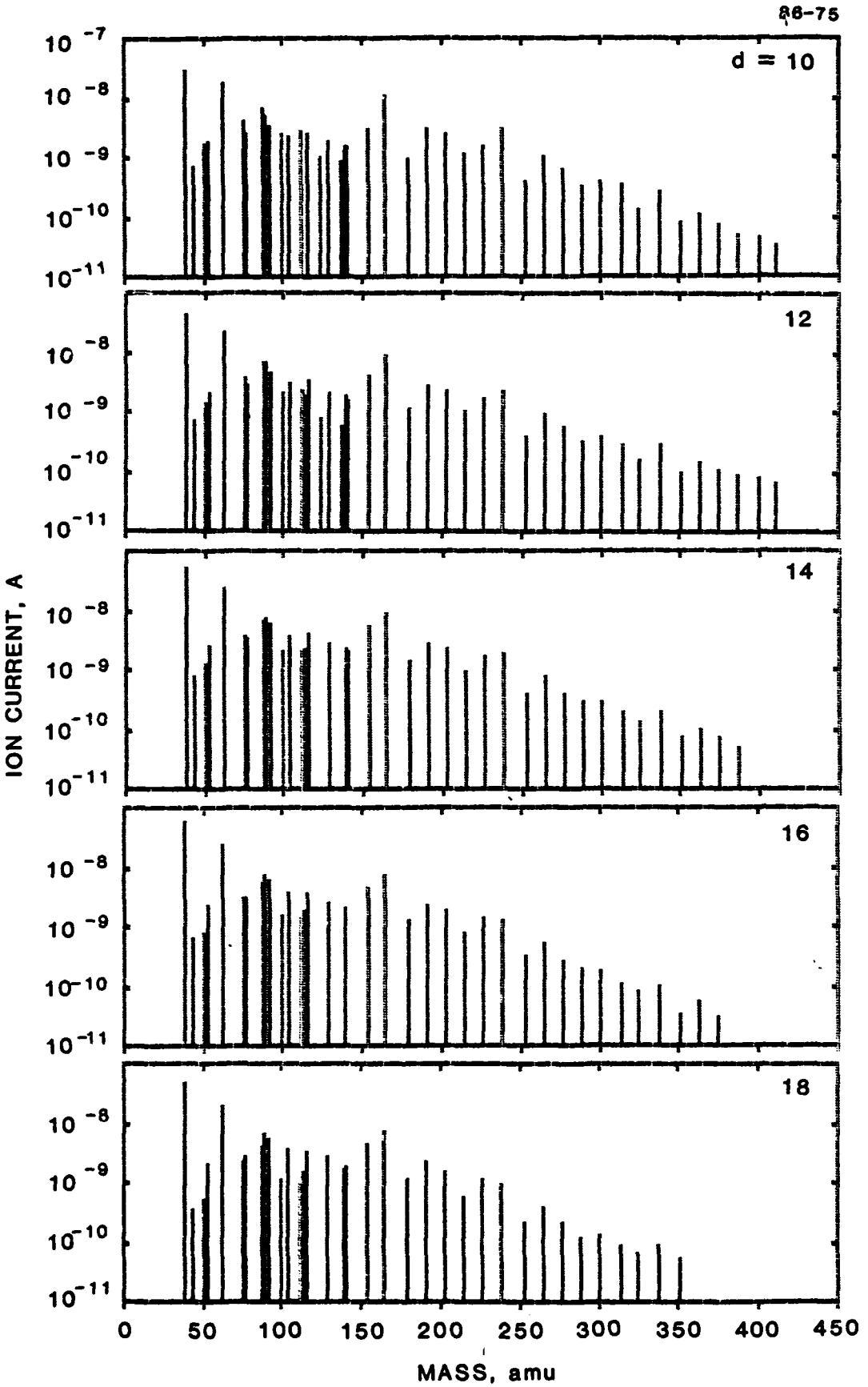
86-75
d = 10
12
14
16
18
ION CURRENT, A
10 -7
10 -8
10 -9
10-10
10-11
0
50
100
150
200
250
300
350
400
450
MASS, amu

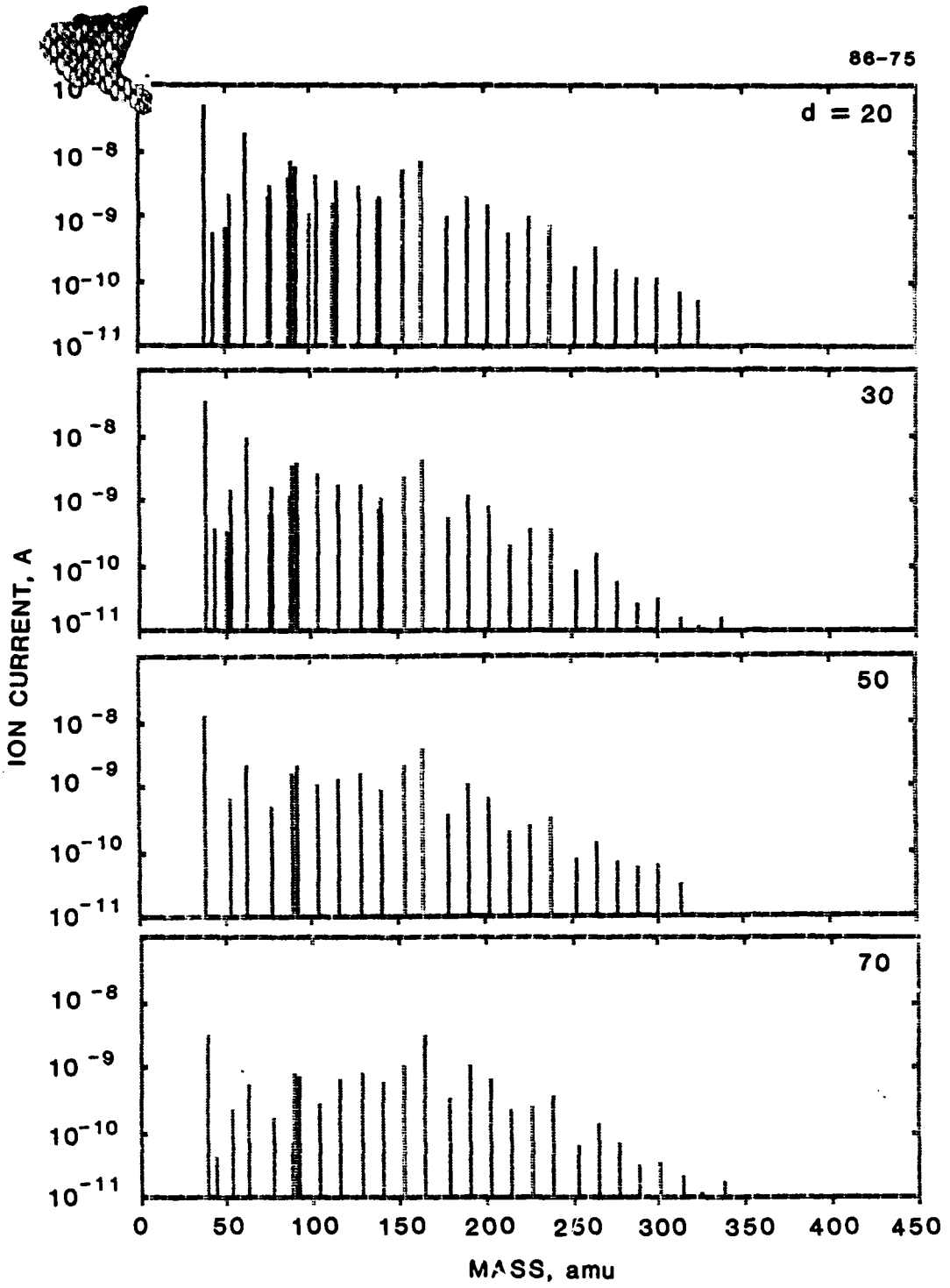

FIGURE 2 ION SPECTRA FOR AN ACETYLENE-OXYGEN FLAME AT THE THRESHOLD FOR SOOT FORMATION

d = height above burner in mm; Ø = 2.5; u = 50 cm s^{-1}; P = 2.67 kPa.

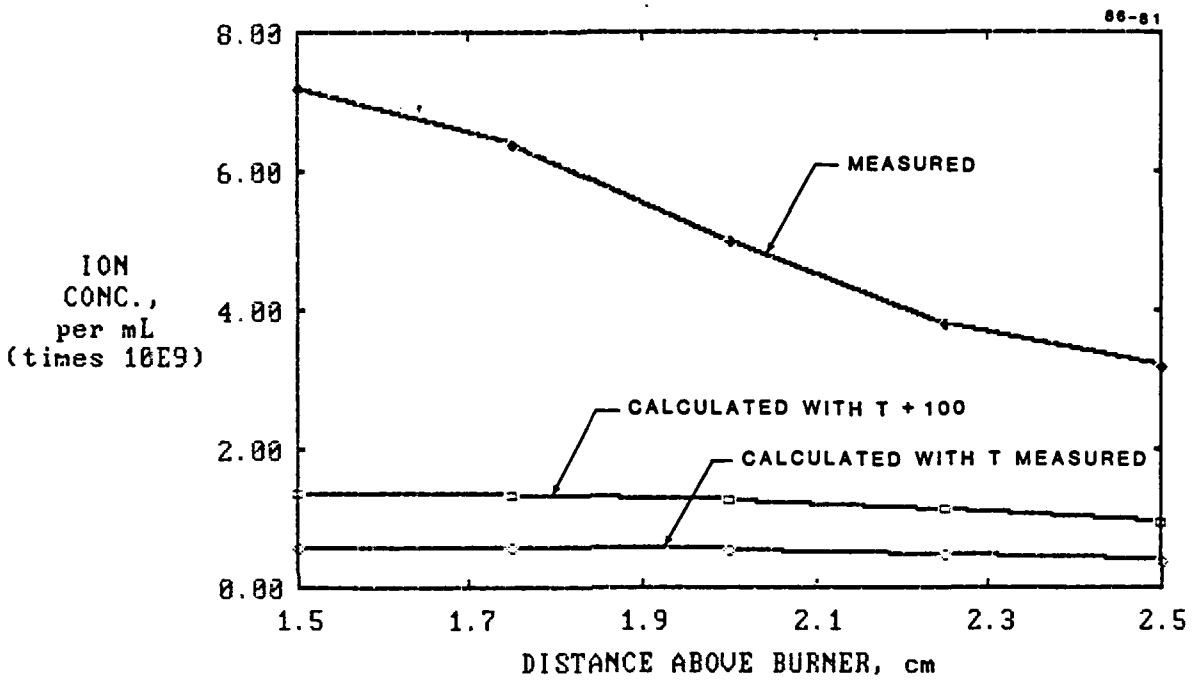

FIGURE 3 MEASURED AND CALCULATED ION CONCENTRATIONS

Comparison of measured ion concentrations in standard low pressure acetylene-oxygen flame (Ø = 3.0, P = 2.67 kPa, u = 50 cm s^{-1})[17] with calculated concentrations for thermally ionized soot particles, with and without 100 K particle heating, in the same flame. Soot concentrations from Homann.[10] Particle diameters in standard flame derived[17] from Homann and coworkers' measurements.[11,12]

END

12-86

DTIC